

AMERICAN UNIVERSITY OF BEIRUT

MOISTURE BUFFERING CAPACITY OF NOVEL SOLAR
REGENERATED HYGROSCOPIC CURTAIN

by
SAMER OMAR SALLOUM

A thesis
submitted in partial fulfillment of the requirements
for the degree of Master of Engineering
to the Department of Mechanical Engineering
of the Faculty of Engineering and Architecture
at the American University of Beirut


Beirut, Lebanon
February 2015

AMERICAN UNIVERSITY OF BEIRUT

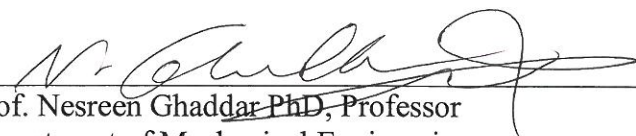
MOISTURE BUFFERING CAPACITY OF NOVEL SOLAR
REGENERATED HYGROSCOPIC CURTAIN

by
SAMER OMAR SALLOUM


Approved by:



Prof. Kamel Abou Ghali, PhD, Professor
Department of Mechanical Engineering
Advisor



Prof. Nesreen Ghaddar PhD, Professor
Department of Mechanical Engineering
Co-Advisor



Prof. Issam Lakkis, PHD, Professor,
Department of Mechanical Engineering
Member of Committee

Date of thesis defense: February 6, 2015

AMERICAN UNIVERSITY OF BEIRUT

THESIS, DISSERTATION, PROJECT RELEASE FORM

Student Name: Salloum Samer Omar
Last First Middle

Master's Thesis Master's Project Doctoral Dissertation

I authorize the American University of Beirut to: (a) reproduce hard or electronic copies of my thesis, dissertation, or project; (b) include such copies in the archives and digital repositories of the University; and (c) make freely available such copies to third parties for research or educational purposes.

I authorize the American University of Beirut, **three years after the date of submitting my thesis, dissertation, or project**, to: (a) reproduce hard or electronic copies of it; (b) include such copies in the archives and digital repositories of the University; and (c) make freely available such copies to third parties for research or educational purposes.



19/02/2014

Signature

Date

ACKNOWLEDGMENTS

I would like to express my sincere appreciation to my advisor Prof. Kamel Ghali for his guidance, support, and advices on my research. I would like to thank him for encouraging my research and for allowing me to grow as a research scientist.

I would also like to thank my co-advisor Prof. Nesreene Ghaddar for her support, guidance and brilliant comments and suggestions.

I would like to thank DR. Issam Lakkis as being a member of my thesis committee

I would also like to thank my parents and my friends for their constant support and motivation.

AN ABSTRACT OF THE THESIS OF

Samer Omar Salloum for

Master of Engineering

Major: Mechanical engineering

Title: Moisture Buffering Capacity of Solar-Regenerated Hygroscopic Curtain.

This study focuses on the potential use of solar energy to actively regenerate a hygroscopic curtain for control the indoor relative humidity. The proposed curtain is supported by a ceiling rotating shaft to allow the curtain material to continuously exchange heat and moisture with the two environments: facing the curtain and the clearance space behind the curtain. As the curtain slowly rotates, one side facing the internal space will undergo absorption while the other side facing the glass surface will undergo desorption releasing the collected space moisture to the exhausted air stream.

In this work a theoretical model is developed from first principles for the proposed system with an integrated indoor space modal to study the rotating hygroscopic curtain feasibility in performing indoor dehumidification. An experimental setup was built inside environmental chambers to validate the theoretical model predictions of room air temperature and moisture removal rate and to test the ability of the rotating curtain to moderate indoor humidity. It was shown that the experimental results for the curtain moisture uptake and the relative humidity inside the chamber compared well with the model simulation results.

A case study was evaluated to predict the effectiveness of a hygroscopic curtain made of cotton and placed in a typical office space in the city of Beirut with a floor area of 42 m². It is found that, for the same conditions, hygroscopic curtain maintain an average relative humidity of about 65.7% when rotating continuously at a speed of 1.5 rpm compared to a value of 71.1% when the curtain is not rotating at all.

CONTENTS

ACKNOWLEDGMENTS.....	v
ABSTRACT.....	vi
NOMENCLATURE.....	ix
LIST OF ILLUSTRATIONS.....	xi
LIST OF TABLES.....	xii
Chapter	
I. INTRODUCTION.....	1
A. Introduction.....	1
B. System description	4
II. MODELING OF MOISTURE BUFFERING BY HYGROSCOPIC ROTATING CURTAIN	7
A. Mathematical Formulation.....	7
1. Moisture and thermal balance of space air enclosure	7
2. Curtain modeling	9
3. Envelope and window modeling	10
B. Numerical solution	11
III. MODEL VALIDATION WITH EXPERIMENT.....	15
A. Experimental setup	13
B. Model validation	16
IV. ASSESSMENT OF THE ROTATING SYSTEM PERFORMANCE.....	18
A. Case study	18

B. Economic analysis of the proposed system vs. conventional vapor compression system.....	24
V. CONCLUSION.....	26
BIBLIOGRAPHY.....	27

NOMENCLATURE

A	surface area,(m ²)
C	heat capacity, (J/kg·K)
h_c	convection heat transfer coefficient at the curtain interface, (W/m ² ·K)
h_{fg}	latent heat of vaporization of the water, (J/kg)
h_{rd}	linearized radiation heat transfer coefficient with the curtain, (W/m ²)
h_w	convection heat transfer coefficient at the wall interface, (W/m ² ·K)
H	curtain height,(m)
K_c	curtain thermal conductivity, (W/m·K)
L	curtain width,(m)
\dot{m}_a	dry air mass flow rate, (kg/s)
\dot{m}_{gen}	moisture generation, (kg/s)
P_c	water vapor pressure in the inter-fiber void space of the curtain, (kpa)
P	water vapor pressure in the air, (kpa)
\dot{Q}_{ent}	internal heat generation, (W)
Q_{solar}	intensity of the solar radiation, (W/m ²)
Q_{sorpt}	heat of sorption, (J/kg)
R	curtain moisture Regain in kg of absorbed water/kg of dry curtain
R_d	curtain dry resistance, (K·m ² / W)
R_e	curtain evaporative resistance, (kPa·m ² / W)
t_c	curtain thickness, (m)
T	temperature, (°C)

T_{mrt} mean radiant temperature in the room, ($^{\circ}\text{C}$)

v curtain velocity, (m/s)

V volume, (m^3)

Greek Symbols

A fraction of solar energy absorbed by the glazing

B convective mass transfer coefficient with vapor pressure as the driving force in ($\text{kg}/\text{kpa}\cdot\text{m}^2\cdot\text{s}$)

Φ relative humidity

ρ density in (kg/m^3)

$(\tau\alpha)$ transmittance absorptance product

Ω Humidity ratio in kg of water vapor/kg of dry air

Subscripts

a_1 air in the indoor space

a_1 air in the air gap space

c_1 curtain side facing indoor air

c_2 curtain side facing window

G Glass

S Supply

ILLUSTRATIONS

Figure		Page
1.	Schematic of the curtains position and its interaction with the room air	5
2.	Three layers of the cloth curtain	6
3.	Simulation flow chart	12
4.	Glass side in front of the curtain	14
5.(a-b)	Comparison of experimentally measured values and model predictions for (a) temperature and (b) humidity ratio of the air in the room	17
6.	A plot of added sensible load and removed latent load as a function of the curtain rotational speed	21
7.	A plot of the average curtain temperature as a function of curtain rotational speed	22
8.	A plot of the average curtain Regain as a function of curtain rotational speed	22

TABLES

Table		Page
1.	Internal loads and Ambient Conditions	19
2.	Room relative and absolute humidity for rpm=0	20
3.	Room relative and absolute humidity for rpm=1.5	23
4.	Energy loads for the Rotating curtain system and Conventional System	25

CHAPTER I

INTRODUCTION

A. Introduction

There are many reasons that justify the need to control humidity and to prevent the indoor relative humidity from exceeding the upper limit of 70% [1, 2]. Human thermal comfort sensation is one of those important reasons [3, 4]. A high relative humidity causes the perspiration rates on the skin to be lower than it should be under dryer conditions. As a result, sweat will accumulate on the human skin triggering a warmer and discomfort feeling. Moreover, research has shown that the indoor relative humidity can significantly affect the perception of IAQ, and thus the needed ventilation rate could possibly be reduced for low relative humidity [5, 6]. Controlling humidity is also important for the building structure as a whole, i.e., increasing the durability of the building structure (wood and steel materials) and prolonging the life service of the building [7]. In fact, Moisture accumulation can degrade building materials through mold growth, rotting, corrosion, and other physical or aesthetic damage [8].

Conventional control of humidity is accomplished by sub-cooling the air to a value less than the dew point temperature; remove a specific amount of the condensate, followed by reheating the air to the required supply temperature. This conventional air conditioning system shows a large destruction of exergy in the evaporator and requires high amounts of electrical energy [9].

Alternatively, one can use desiccant dehumidification as less energy requiring process [10, 11, and 12].

Both processes require energy to control the level of humidity and therefore both are classified as active methods for controlling the humidity. In the first process, not only the air-conditioning system has to be oversized to meet the sub-cooling requirement of the latent load, but also the operational energy of the air-conditioning system is increased due to the excess cooling and reheating. In the second process, liquid/solid hygroscopic materials are employed to absorb the excess moisture and the regeneration of the desiccant material is accomplished by applying thermal energy. The classification of whether this process is considered an active or a passive method depends on whether energy is used in removing the humidity. If it requires reactivation heater, the method is considered active and if it operates naturally then it is considered as a passive way. [13]

The continuous increase in energy demand and costs pushed researchers to study the hygroscopic moisture capacity of the different building materials as passive techniques for controlling indoor humidity [14,15]. The literature studies concluded that the use of some building materials has the ability to moderate the indoor relative humidity during the different seasons. For example, Simonson et al. [16] showed that the wooden materials inside bedrooms can reduce the peak humidity by 35% when the ventilation rate is 0.5 ACH. The numerical study of Cerolini et al. [17] has shown that that the cellulose based material have a higher buffering performance and a faster adjustments to variations in indoor relative humidity when compared to non-cellulosic common building materials. Hameury et al. [18] showed that the porous timber structures of floor and walls have an appreciable effect on buffering indoor humidity levels. Other researchers considered the use of household materials cloth curtains, carpets, and wallpaper to assist the air-conditioning system in eliminating the problems associated with high humidity levels. Through absorption and desorption, hygroscopic materials in the indoor environment are able to dampen the moisture variations

of the indoors air [19]. During high latent loads, hygroscopic materials reduce the peaks of relative humidity levels due to their absorbing characteristics, and during small latent load their desorption characteristics allow them to release the previously absorbed moisture into the indoor air, and thus keeping a more uniform indoor humidity level. Therefore, household hygroscopic materials buffer the moisture variation in a passive way and moderate the variation of indoor humidity. In particular, Ghali et al. [20] investigated the indoor moisture moderating capacity of cloth curtains during the part load operation of a DX air conditioning system. The study showed that cotton hygroscopic curtain was capable of restricting the indoor relative humidity between 44% - 65% as compared to a relative humidity range of 40% - 70% when no curtain was used. However, in the absence of any active method for regenerating the hygroscopic curtain, its success in moderating the indoor moisture not only depends on its hygroscopic capacity but also on the building latent load profile and the air conditioning system operation. The on-off operation of the DX air conditioning system during uniform latent load are essential for the effective moisture buffering of a curtain in the absence of active regeneration.

It is evident that the hygroscopic building construction materials can buffer the building indoor moisture during different seasons whereas the indoor household hygroscopic materials moderate the daily indoor relative humidity during transient changes of indoor latent load. However, such studies have limited application for office buildings characterized by uniform latent load and constructed from non-cellulosic structural material. One solution is to consider active regeneration methods of the curtain. Solar energy presents potential source to actively regenerate cloth curtains to allow the hygroscopic curtain to control the indoor relative humidity. A rotating mechanism for a curtain mounted close to a glazing surface is proposed to assist in controlling the indoor relative humidity of a typical office. Hence, the

objectives of the work are to develop a mathematical model capable of predicting the rotating curtain absorption and regeneration behaviour and validate the model prediction on moisture uptake and removal with experiments. A case study of an office located in the coastal city of Beirut will follow to show the feasibility of using the rotating hygroscopic curtain system to control humidity

B. System description

The proposed hygroscopic solar-regenerated rotating curtain system is shown in Fig. 1. The curtain is supported by the ceiling-mounted rotating shaft to allow the curtain material to continuously exchange heat and moisture with the two environments: facing the curtain and the clearance space behind the curtain. Thus at each time, one part of the curtain will be facing the window and is heated by solar radiation while the other part is facing the indoor room and is cooled by convection.

The air conditioning system of the office space consists of a supply grill placed in front of the curtain while the exhaust grill is located behind the curtain in the clearance space between the wall and the curtain. To prevent air short-circuit, air from the wall facing the curtain will be withdrawn and transported behind the curtain to be exhausted from the ceiling grill (see Fig. 1).

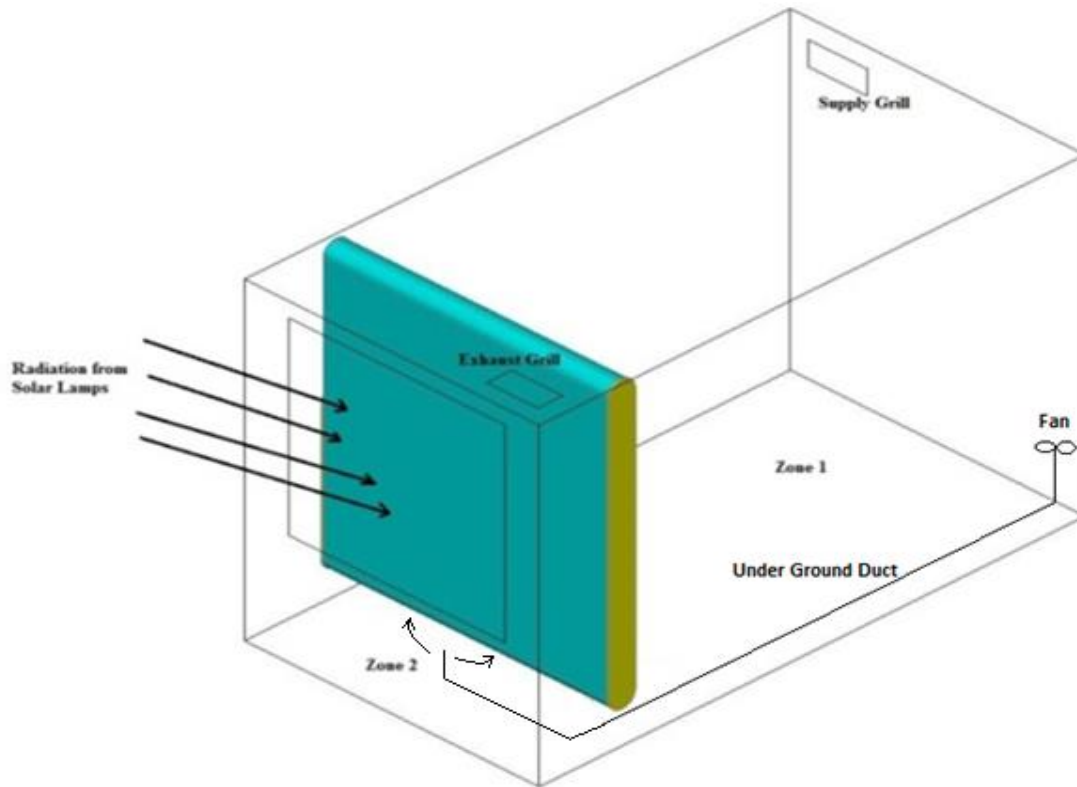


Figure 1: Schematic of the curtains position and its interaction with the room air

The curtain is made mainly from hygroscopic material absorbing moisture from the indoor environment and desorbing the moisture to the exhausted air. To prevent heat and moisture exchange between the two sides (absorbing and desorbing), the cloth curtain will consist of the following layers: hygroscopic cloth layer, nonconductive fabric layer and impermeable membrane between these two layers as shown in Fig. 2. To further reduce heat flow from the moisture absorbing curtain side towards the regenerating curtain side, an insulating layer made of Styrofoam will be placed between the curtain sides (see Fig. 2).

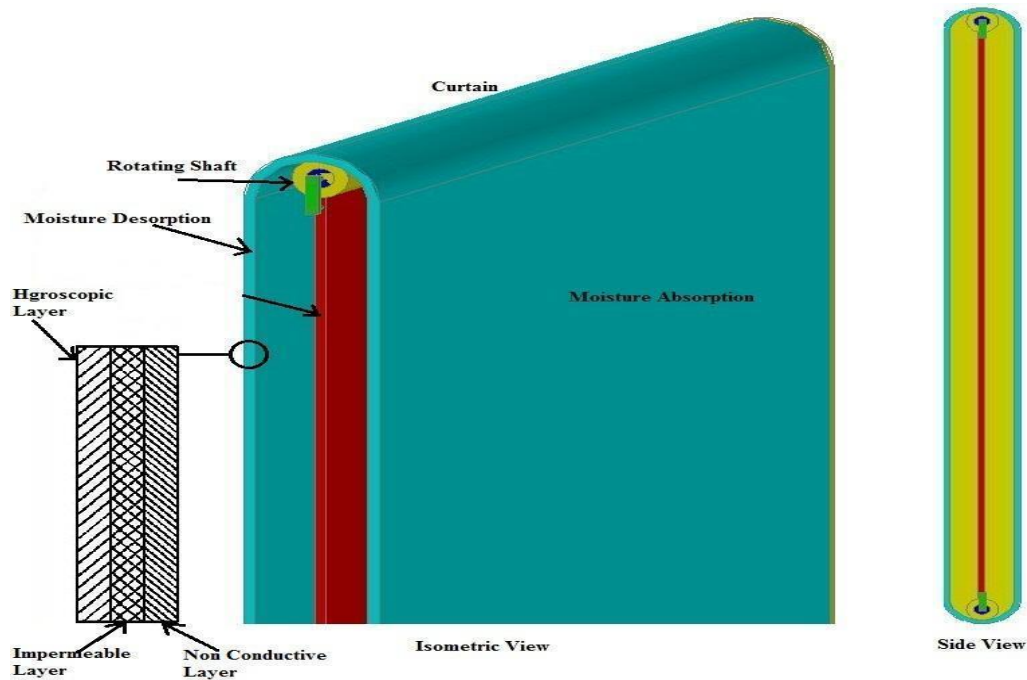


Figure 2: Three layers of the cloth curtain

As the curtain slowly rotates, one side facing the internal space will undergo absorption while the other side facing the glass surface will undergo desorption releasing the collected space moisture to the exhausted air stream.

A mathematical model for a rotating curtain placed in front of a large glass wall is developed to assess the moisture buffering capacity of cloth curtain regenerated by solar energy. The curtain model will be coupled with the space thermal model and air conditioning system to predict the curtain ability in controlling indoor relative humidity. The coupled heat and moisture balance equations will be solved numerically. This step is then followed by performing experiments inside climatic chambers located in the energy lab at the American University of Beirut (AUB) to validate the numerical results of the developed model. A final section is then presented for a case study showing the feasibility and effectiveness of using the hygroscopic curtain in a typical office located in Beirut warm humid climate

CHAPTER II

MODELING OF MOISTURE BUFFERING BY HYGROSCOPIC ROTATING CURTAIN

A. Mathematical Formulation

The mathematical models will couple energy and moisture balances of space air enclosure and the rotating curtain layer as well as the energy balances of the facing window and room walls.

1. Moisture and thermal balance of space air enclosure

Curtains are usually placed in front of a glazing surface for solar shading purposes dividing the space air into two distinct zones (see Fig. 1): air space facing the curtain from one side (zone 1) and air volume behind the curtain from its other side (zone 2). It is to be noted that since the curtain is rotating the moisture content along its two sides (absorbing and desorbing) are not uniform.

The energy balance equations for the air in zones 1 and 2 are given by:

$$\rho_a V_{a1} C_{a1} \frac{\partial T_{a1}}{\partial t} = \sum_{i=1}^{i=5} h_{wi} A_{wi} (T_{wi} - T_{a1}) + \int_0^H \frac{L\{T_{c1}(z,t) - T_{a1}\}}{1/h_{c1} + R_d/2} dz + \dot{Q}_{ent} + \dot{m}_a C_s (T_s - T_{a1}) \quad (1)$$

$$\rho_a V_{a2} C_{a2} \frac{\partial T_{a2}}{\partial t} = \int_0^H \frac{L\{T_{c2}(z,t) - T_{a2}\}}{1/h_{c2} + R_d/2} dz + \dot{m}_a C_{a1} (T_{a1} - T_{a2}) + h_{cg} A_g (T_g - T_{a2}) \quad (2)$$

In Eq. (1), the term on the left hand side of the equation accounts for the thermal capacitance of the air stored in zone 1. The four terms on the right hand side of the equation represent the heat transfer exchange with the five surfaces (3 walls, ceiling, and floor), the heat transfer

exchange with the curtain, the internal energy released, and the energy exchange through the air mass flow rate into the room respectively. The energy balance equation for zone 2 (Eq. (2)) is very similar to that of zone 1 except that it does not include the internal energy released.

The surface wall temperature is denoted T_w , A_w is the surface area of a wall, and h_{cw} is the corresponding convective heat transfer coefficient. The temperatures T_{a1} and T_{a2} are the air dry bulb temperature of the air trapped in zone 1 and 2 respectively; T_{c1} and T_{c2} are the curtain temperatures at both sides; and T_s is the supply air dry bulb temperature. The air-vapor mixture heat capacity per kilogram of dry air in zone 1 and 2 are C_{a1} and C_{a2} respectively; C_s is the supply the air-vapor mixture heat capacity per kilogram of dry air; ρ_a is the dry air density, and \dot{m}_a is the dry air mass flow rate. The curtain width and height are L and H respectively; V_{a1} and V_{a2} are zone 1 and 2 space volume; R_d is the curtain dry resistance, h_{c1} and h_{c2} are the convective heat transfer coefficients on both sides of the curtain

The moisture conservation equations for both zones are given by

$$\rho_a V_{a1} \frac{\partial \omega_{a2}}{\partial t} = \dot{m}_{gen} + \dot{m}_a (\omega_s - \omega_{a1}) + \int_0^H \frac{L \{P_{c1} - P_{a1}\}}{\frac{1}{\beta_1} + \frac{h_{fg} R_e}{2}} dz \quad (3)$$

$$\rho_a V_{a2} \frac{\partial \omega_{a2}}{\partial t} = \dot{m}_a (\omega_{a1} - \omega_{a2}) + \int_0^H \frac{L \{P_{c2} - P_{a2}\}}{\frac{1}{\beta_2} + \frac{h_{fg} R_e}{2}} dz \quad (4)$$

Where ω_{a1} and ω_{a2} are the air humidity ratio in zone 1 and 2, ω_s is the supply air humidity ratio, and P_{c1} and P_{c2} are the vapor pressure in the inter-fiber air void space of the curtain which are derived from the experimental isotherm equilibrium curve; β_1 and β_2 are the convective mass transfer coefficient with vapor pressure as the driving force and are obtained

from the Lewis relation, R_e is the evaporative resistance of the curtain and h_{fg} is the latent heat of vaporization.

2. Curtain modeling

The Eulerian method is used to model the Temperature and moisture content of the curtain. A fixed control volume is chosen, and the temperature and moisture content variations are derived for this specific control volume. The temperature and moisture content are assumed to be uniform throughout any horizontal section. Thus an unsteady one dimensional (t, z) model is derived for Temperature and moisture fields for the curtain facing each zone

The energy balance equations for sides 1 and 2 of the curtain are given by equations (5) and (6) respectively as follows:

$$\rho_c t_c C_c \left\{ \frac{\partial T_{c1}}{\partial t} + v \frac{\partial T_{c1}}{\partial z} \right\} = K_c t_c \frac{\partial^2 T_{c1}}{\partial z^2} + \frac{T_{a1} - T_{c1}}{\frac{1}{h_{c1}} + \frac{R_d}{2}} + \frac{P_{a1} - P_{c1}}{\frac{1}{\beta_1} + \frac{h_{fg} R_e}{2}} Q_{sorp1} + h_{rd-1} (T_{mrt-1} - T_{c1}) \quad (5)$$

$$\rho_c t_c C_c \left\{ \frac{\partial T_{c2}}{\partial t} - v \frac{\partial T_{c2}}{\partial z} \right\} = K_c t_c \frac{\partial^2 T_{c2}}{\partial z^2} + \frac{T_{c2} - T_{c1}}{\frac{1}{h_{c2}} + \frac{R_d}{2}} + \frac{P_{a2} - P_{c2}}{\frac{1}{\beta_2} + \frac{h_{fg} R_e}{2}} Q_{sorp1} + h_{rd-2} (T_g - T_{c2}) + (\tau\alpha) Q_{solar} \quad (6)$$

Where ρ_c is the curtain density, C_c is the curtain specific heat capacity of the curtain which is a function of the curtain regain, t_c is the curtain thickness, V is the curtain velocity, Q_{sorp1} is the released heat of sorption, Q_{solar} is the intensity of the solar radiation and T_g is the glass or window temperature, h_{rd} is the linearized radiation heat transfer coefficient with the curtain, T_{mrt-1} is the mean radiant temperature in the room and $(\tau\alpha)$ is the transmittance absorptance product.

The moisture conservation equations for both sides curtain are given by

$$\rho_c t_c \left\{ \frac{\partial R_{c1}}{\partial t} + v \frac{\partial R_{c1}}{\partial z} \right\} = \rho_c t_c D_c \frac{\partial^2 R_{c1}}{\partial z^2} + \frac{P_{a1} - P_{c1}}{\frac{1}{\beta_1} + \frac{h_{fg} R_e}{2}} \quad (7)$$

$$\rho_c t_c \left\{ \frac{\partial R_{c2}}{\partial t} - v \frac{\partial R_{c2}}{\partial z} \right\} = \rho_c t_c D_c \frac{\partial^2 R_{c2}}{\partial z^2} + \frac{P_{a2} - P_{c2}}{\frac{1}{\beta_2} + \frac{h_{fg} R_e}{2}} \quad (8)$$

Where R_{c1} and R_{c2} are the curtain moisture regain at both sides. Note that the regain R has a definite relation to the relative humidity of the water vapor through a property curve of the regain versus relative humidity, Morton et al. [21].

3. Envelope and window modeling

The thermal response of the envelope is modeled as a simple lumped resistance–capacitor element to obtain the inner wall surface temperature, based in the work of Laret et al. [22] and implemented in the study of Ghali et al [20].

Assuming a uniform Temperature for the window, the energy balance can be written as:

$$\rho_g t_g \frac{\partial T_g}{\partial t} = h_{rd-2} (\bar{T}_{c2} - T_g) + h_{c2} (T_{a2} - T_g) + h_{rco} (T_{amb} - T_g) + \alpha Q_{solar} \quad (10)$$

Where \bar{T}_{c2} is the average temperature of the curtain facing the window, T_{amb} is the outside ambient temperature, h_{rco} is the combined convective and radiative heat transfer coefficient between the glass and the outside surrounding, and α is the fraction of solar energy absorbed by the glazing

B. Numerical solution

To simulate the buttering capacity of the solar regenerated rotating curtain, the following input information is needed: building envelope construction material, external and internal load profiles, the material and physical properties of the hygroscopic curtain (evaporative and dry resistances and regain curve function of relative humidity). The calculation domain at both sides of the curtain (absorbing and desorbing) is divided into a number of non-overlapping control volumes such that there is two control volumes surrounding each grid point. Each side of the curtain is subdivided into n sections of equal thickness Δz resulting in a total of $n + 1$ grid points in the z -dimension along each curtain side.

Starting from arbitrary initial conditions of a typical summer day and using a time step of 1 s for the explicit scheme, the temperature and moisture fields along the curtain length was calculated assuming a stepwise upwind profile. Figure 3 shows the simulation flowchart and model inputs.

The curtain temperature and moisture fields were used in the space model to determine the indoor temperature and relative humidity. At the end of the 24 h operational period, the initial conditions are recalculated and used as input in the cyclic simulations until steady periodic convergence is achieved. The criteria for convergence is reached when the maximum percentage errors for the curtain temperature, air temperature, air humidity content in either zone, and the regain values are all less than 10–4% when values at time t and $t + 24$ h are compared. Different time steps are chosen for the simulation: 1 and 0.1 s over the whole simulation period. The higher time step of 1 s is found sufficient to produce a stable accurate

solution. The curtain on both sides was discretized to 20 control volumes; i.e. $\Delta z = 0.05 \text{ m}$ for a 1.0 m curtain height

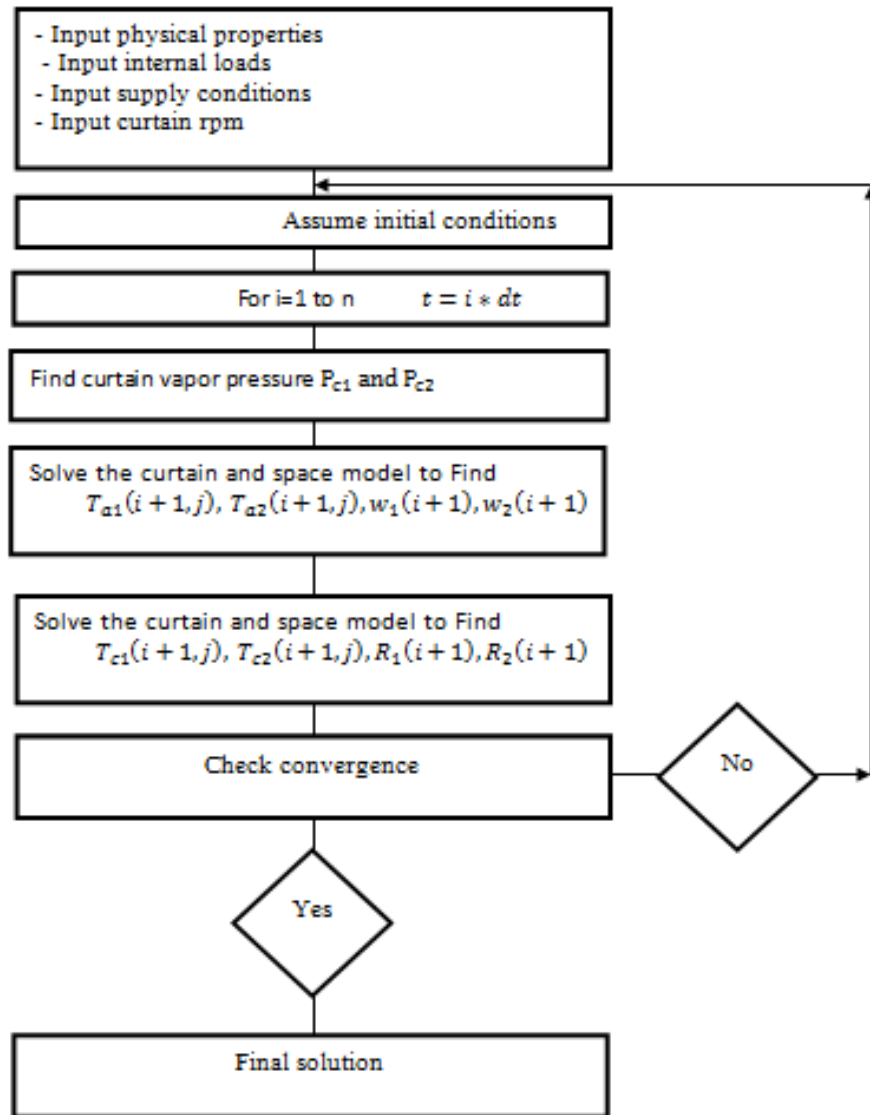


Figure 3: Simulation flow chart

CHAPTER III

MODEL VALIDATION WITH EXPERIMENT

A. Experimental setup

An experimental setup was built inside the climatic chamber of AUB to test the ability of the hygroscopic rotating curtain in performing indoor dehumidification and to validate the numerical results of the theoretical model. The experimental chamber has an area $1.0 \text{ m} \times 1.1 \text{ m}$ and a height of 1.0 m . It consists of one fully glazed facade having an area of $1.0 \times 1.1 \text{ m}$ which is exposed to solar radiation while the other three walls along with the floor and ceiling are partitioned with conditioned spaces. The walls, floor, and ceiling of the chamber are made of Styrofoam and are well insulated with metallic sheet coverings on both sides of the wall to prevent moisture migration through the walls. An artificial solar radiation panel source was placed in front of the glazed facade (4 mm thick commercial window glass) in order to simulate the sun radiation and thus to heat the curtain. The radiant heating source is composed of a set of six halogen lamps rated at 1000W each ($1 \text{ m} \times 1 \text{ m}$) placed vertically and backed with parabolic reflectors. The power input to the lamp is monitored for stable non-fluctuating operation. A special CM3 Campbell Scientific Pyranometer of spectral range $305\text{-}2800 \text{ nm}$ is used to measure the radiative heat flux from the Halogen lamps at different locations on the glazed window. The spectral selectivity of the Pyranometer is $\pm 5\%$ ($350\text{-}1500 \text{ nm}$), with a sensitivity of 10 to $35 \mu\text{V}/\text{Wm}^2$ and impedance of 60 to 200 Ohm . The solar panel is calibrated through dimmer so that the solar flux hitting the outer surface of the glazing is equal to $700 \text{ W}/\text{m}^2$. A curtain having an area of $1.0 \text{ m} \times 1.0 \text{ m}$ is placed behind the glazed facade at a distance of 10 cm as shown in Fig. 4.



Figure 4: Glass side in front of the curtain

The curtain is mounted on two parallel shafts that are controlled by an AC motor to allow its rotation at a constant speed of 1.5 rpm. The used curtain is 100% untreated cotton having the following properties: thickness 0.41 mm, dry thermal resistance of $0.0158 \text{ }^\circ\text{C m}^2/\text{W}$ and evaporative resistance of $4.28 \text{ Pa}\cdot\text{m}^2/\text{W}$ measured by a sweating guarded hot plate (SGHP-8.2) in accordance with ASTM F1868 [23] and ISO 11092 [24] to measure both R_{et} (thermal) and R_{ev} (vapor) characteristics .

The indoor space is conditioned by 100 % fresh air that enters the experimental chamber at an average temperature and relative humidity of 25 C and 46% respectively. A controlled suction fan is place within a duct to ensure proper air flow from the surrounding conditioned partition. Another identical fan, placed on the ceiling between the curtain and the glazed façade, is used as an exhaust to allow air flow outside the room. The fans are powered by an

alternating current supply having a voltage of 220V. The mass flow rate of the air was calculated through measuring the velocity through an anemometer (BK PRECISION model 731A), with error of 3.0% of the reading. The air mass flow rate was set at $0.016 \text{ m}^3/\text{s}$ by controlling the speed of the suction fans. Two humidifiers were placed in the middle of the chamber releasing steam at a rate of 0.23 g/s . This rate was measured experimentally from the humidifier rate of water loss. OMEGA[®] HX94A Series humidity-Temperature sensors with relative humidity accuracy of $\pm 2.5\%$ and temperature accuracy of $\pm 0.3^\circ\text{C}$ were used to monitor the temperature and relative humidity during experimentation. The sensors were placed at the inlet of the supply duct and in the middle of the experimental chamber and the sensor temperature and humidity readings were simultaneously recorded via a data acquisition system every one minute.

Heat gains in the room due to the steam generation and to the solar radiation that by-pass through the clearance between the wall and curtain was estimated at a 200 W value by running the experiment under the constant air supply conditions, uniform moisture generation, solar lamps on and the non-rotating curtain until steady state conditions were attained (4 hours). The experimental protocol for measuring the ability of a solar regenerated curtain to control the indoor humidity was conducted for a total period of 4 hours. In the first 2 hour period, the curtain was rotating at a constant speed absorbing moisture from the indoors and releasing the moisture with the exhausted air and in the remaining four hours period the rotating motor was stopped.

B. Model validation

The integrated model of the rotating hygroscopic curtain system was simulated for the geometric and physical parameters of the experiment while using the experimentally measured average inlet conditions as inputs to the model. The predictions of the mathematical model and the actual experimental measurements of the room temperature and humidity are shown in Fig. 5 (a-b). As it can be seen, the model was able to closely predict the steady state response of the room temperature and humidity when the motor was on and off. The error in predicting the steady state room temperature was about 2%. As for the relative humidity, the error was about 4%. As also shown in Fig. 5(a) and Fig. 5(b), the rotating curtain, while removing part of the latent load, will add some sensible load to the room. In fact, when the curtain was rotating, the steady state humidity ratio was about 0.026 versus a value of 0.027 when the motor was off. Therefore, the rate of moisture absorbed by the rotating curtain is 1.9×10^{-5} kg/s and the latent load is reduced by

$$Q_{\text{lat}} = \dot{m}_a (0.027 - 0.026) h_{\text{fg}} = 42.9 \text{ W} \quad (11)$$

On the other hand when the curtain was rotating, the steady state temperature was about 36°C versus a value of 34°C when the motor was off. This increase in the steady state temperature ascertains the fact that the rotation of the curtain increases the sensible load by

$$Q_{\text{sens}} = \dot{m}_a C_{\text{po}} (36.0 - 34.0) = 39.2 \text{ W} \quad (12)$$

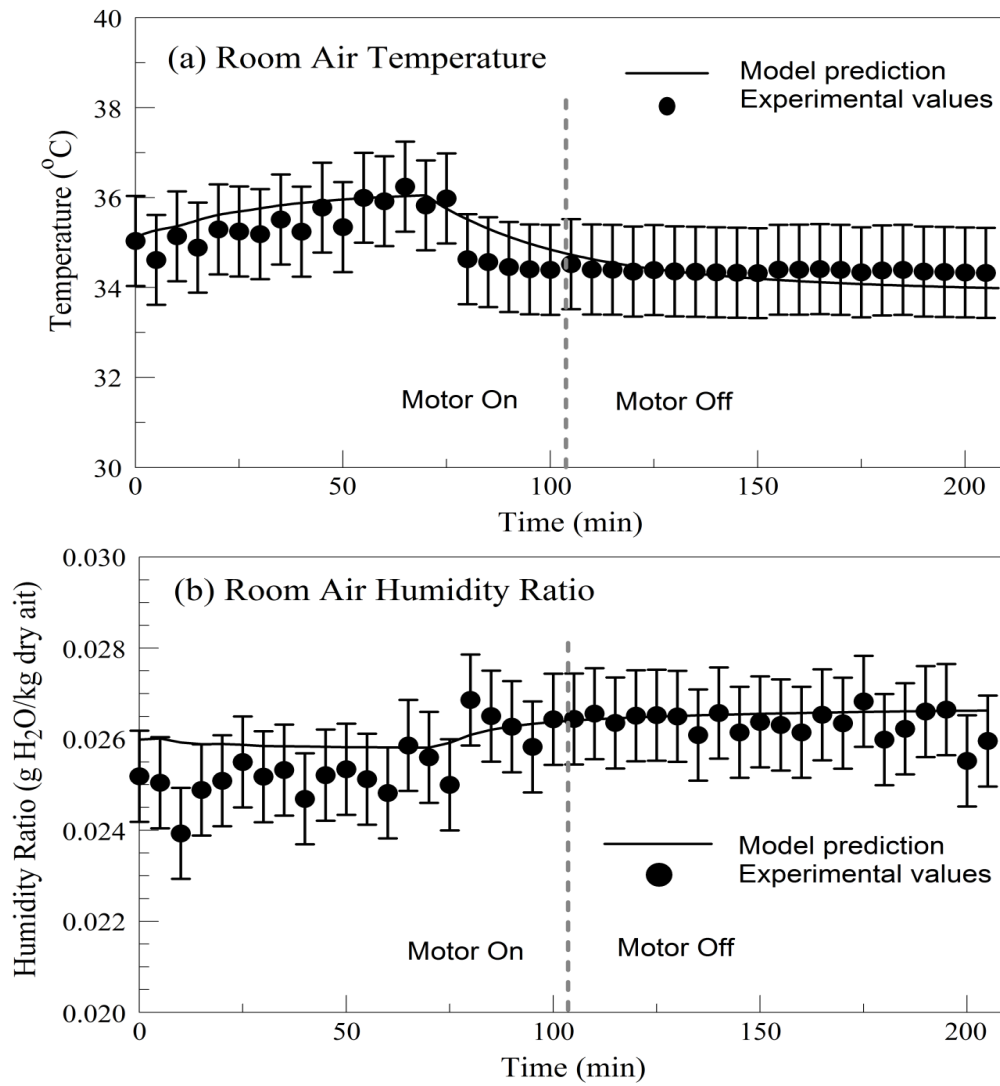


Figure 5(a-b)

Figure 5 (a-b): Comparison of experimentally measured values and model predictions for (a) temperature and (b) humidity ratio of the air in the room

CHAPTER IV

ASSESSMENT OF THE ROTATING SYSTEM PERFORMANCE

A. Case study

The proposed study aims to assess the performance of the rotating hygroscopic curtain placed in a typical office space in the city of Beirut with a $6\text{ m} \times 7\text{ m}$ floor area and 3.5 m ceiling height. As mentioned earlier, Beirut is a coastal city; hence sea water can be used as a heat sink to supply the required cooling loads. The sink temperature is low ($17\text{ }^{\circ}\text{C}$) to cool the flow of outdoor air entering the occupied space but it is not low enough to control the indoor humidity. A hygroscopic curtain made of 100% untreated cotton is supported by a ceiling rotating shaft to allow its rotation in front of a glass area of 21 m^2 on the south façade of the office and exposed to solar radiation. The rotating curtain will continuously absorb moisture from its side that faces the indoor space and will reject the accumulated moisture to the exhaust air leaving the space from the other side facing the glazing.

The office is occupied from 8:00 a.m. till 5:00 p.m. and the internal loads (sensible and latent) along with the ambient conditions of a typical summer day in Beirut (August 15) are presented in Table 1. The indoor space is conditioned by 100 % fresh air. Deep sea water at 17°C is used as a heat sink to lower inlet air temperature to 18°C [25]. For a typical summer day in Beirut, the dew point temperature of the ambient air is higher than 18°C . Hence, the supply air will enter at 100% relative humidity and at humidity ratio of 12.93 g of H_2O /kg of dry air.

Time of the day	Internal loads(W)		Ambient conditions		
	Sensible	Latent	Temp. (°C)	Humidity Ratio (g/kg)	Solar Flux (W)
8:00-9:00	987	128	29	17.02	512
9:00-10:00	987	128	30	18.06	653
10:00-11:00	987	128	30	18.06	754
11:00-12:00	1554	256	31	19.15	798
12:00-13:00	1554	256	31	19.15	780
13:00-14:00	1554	256	30	18.06	701
14:00-15:00	1392	220	31	19.15	574
15:00-16:00	1392	220	31	19.15	419
16:00-17:00	1392	220	31	19.15	256

Table 1: Internal loads and Ambient Conditions

The model is simulated for a representative day in August (15th of the month) for the case of a non rotating curtain. The corresponding supply air flow rates, needed to maintain room temperature around 24°C, are shown in Table 2. The simulation results show that the free cooled air was able to maintain a good comfort temperature but not a good relative humidity. In fact, for the mass flow rate of conditioned air shown in Table 2, the average value of the humidity ratio was 13.35 g/kg, which was higher than the supply air humidity ratio of 12.93 g/kg due to the latent load in the space. The humidity ratio reached a peak of 13.39 g/kg at noon hour, when the latent load was the highest. The corresponding relative humidity was on average 71.1%, ranging between 70.5 and 71.5%. Moreover, increasing the mass flow rate of air entering the office will not resolve the issue of high humidity, thus the saturated free

cooled air cannot alone satisfy human thermal comfort due to the high relative humidity.

Hence, an auxiliary system that can handle part of the office latent load is needed.

	Supply air flow rate (m ³ /s)	% Relative humidity	Humidity ratio (g/kg)
8:00-9:00	0.13	70.5	13.31
9:00-10:00	0.13	70.5	13.31
10:00-11:00	0.13	70.5	13.31
11:00-12:00	0.21	71.52	13.39
12:00-13:00	0.21	71.52	13.39
13:00-14:00	0.21	71.52	13.39
14:00-15:00	0.19	71.3	13.35
15:00-16:00	0.19	71.3	13.35

Table 2: Room relative and absolute humidity for rpm=0

To assess the performance of the rotating hygroscopic curtain in moderating the indoor humidity, it is important to select the optimal rotating speed of the curtain at which the curtain will decrease indoor moisture without excessively increasing the sensible load. To this end, the curtain model will be simulated at the peak latent load hour (11:00- 13:00) for different curtain rotational speeds. Figure 6 shows both the decrease in latent load and the increase of the sensible load at different curtain speeds.

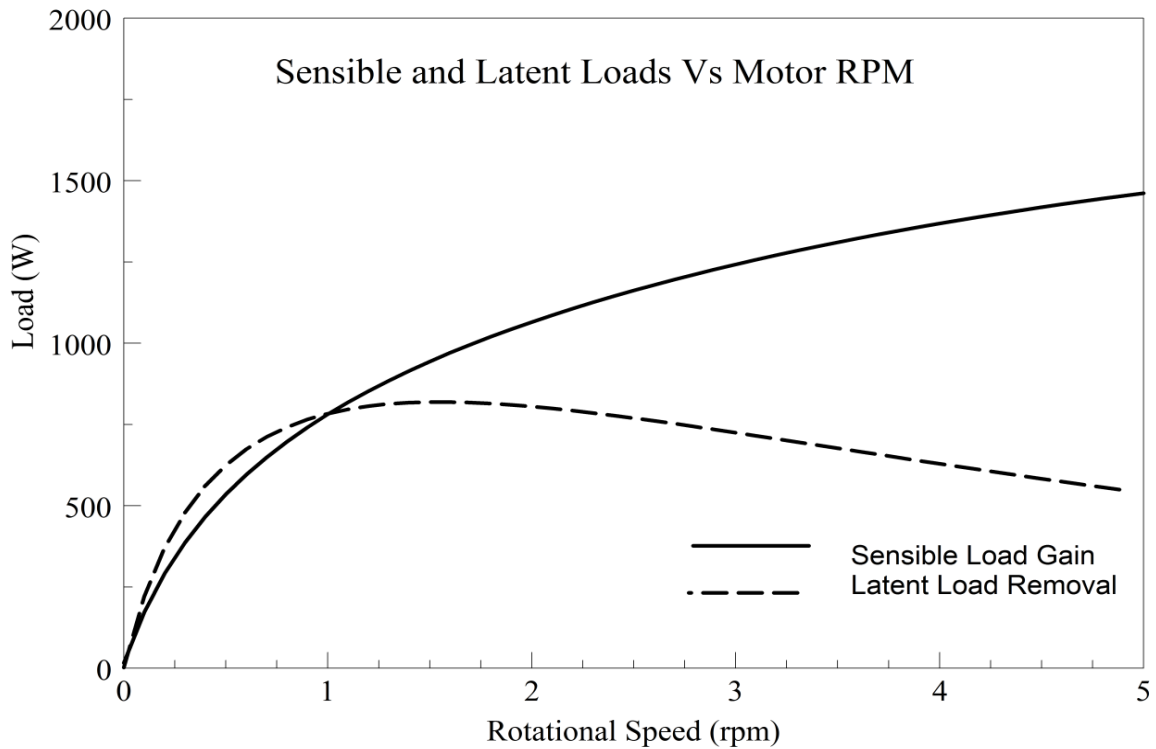


Fig. 6

Figure 6: A plot of added sensible load and removed latent load as a function of the curtain rotational speed

As the curtain rpm increases, the added sensible load always increases due to the increase of the average temperature of the curtain facing the rom. However latent load removal increases and reaches a maximum of 819W at an rpm =1.5 after which it began to decrease. In fact, the mass flow rate of water vapor absorbed by the curtain increases as the average curtain temperature and regain decreases. Nevertheless, as shown in Figure 7 and 8, boosting the curtain speed will result in an increase in curtain temperature and a decrease in curtain regain which explains the presence of an optimum rpm that maximize the latent load removal. Moreover, the added sensible, which is to some extent higher the removed sensible load for an rpm of 1.5, can be easily handled by increasing the mass flow rate of cooled air using the

available heat sink water without any additional cost. Thus an optimal rpm of 1.5 will be chosen throughout the simulation.

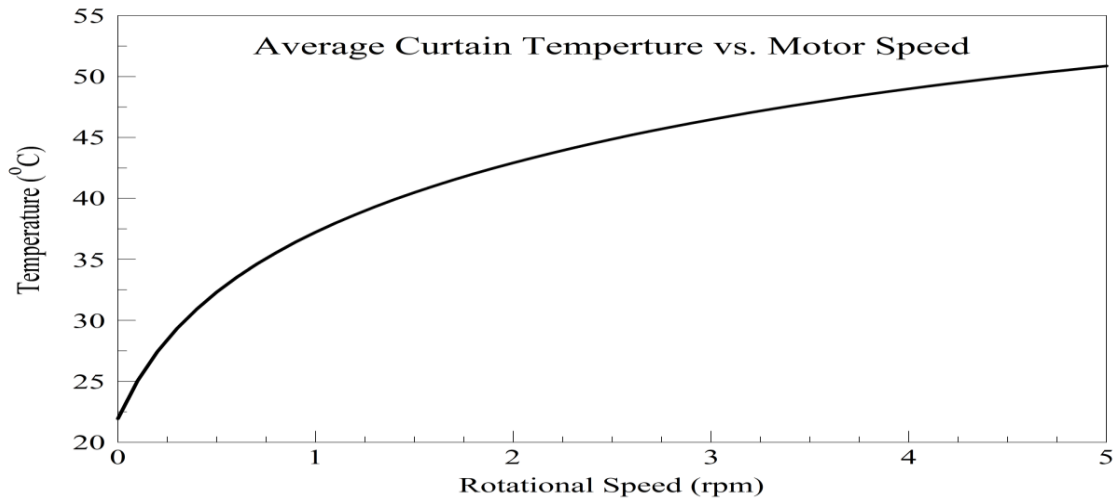


Fig. 7

Figure 7: A plot of the average curtain temperature as a function of curtain rotational speed

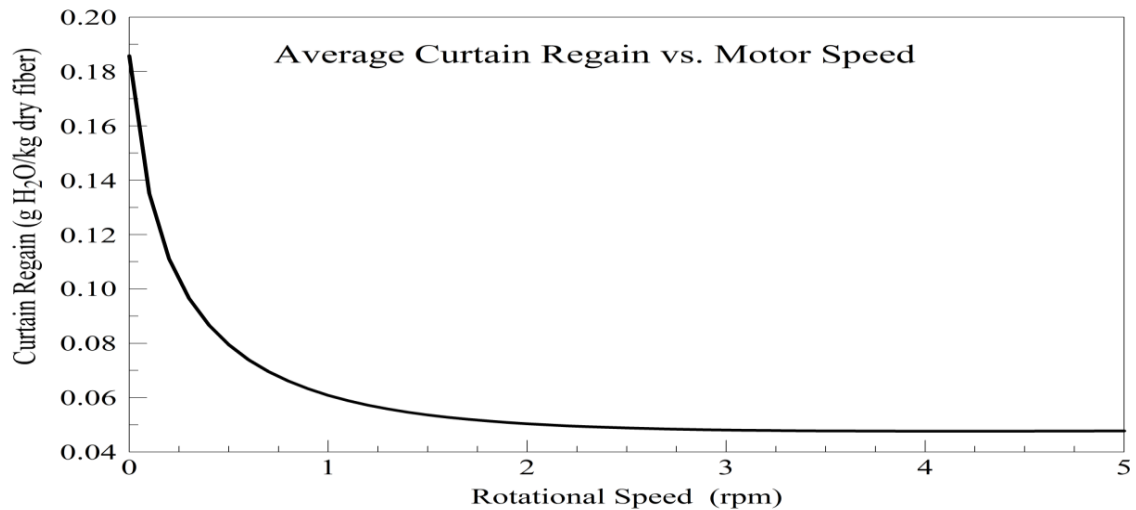


Fig. 8

Figure 8: A plot of the average curtain Regain as a function of curtain rotational speed

To counter effect the additional sensible load and to restore a comfortable temperature of 24°C, the air flow rate of free cooled outdoor air is increased. The corresponding new supply air flow rates needed to maintain room temperature around 24°C when the curtain is rotating at an rpm of 1.5 is shown in Table 3. The simulation results show that the new supplied air flow rates with the rotating curtain are to maintain a good comfort temperature and relative humidity. In fact, the average value of the humidity ratio dropped from 13.35 g/kg to 12.3 g/kg when the curtain is rotating at an rpm of 1.5. The average indoor air relative humidity has decreased to an average value of 65.83% as compared to a value of 71.1% when the curtain is not rotating. The relative humidity is ranging between 63.97% and 68.37% which is comfortable for most people.

	Supply air flow rate (m ³ /s)	% Relative Humidity	Humidity ratio (g/kg)
8:00-9:00	0.24	65.2	12.13
9:00-10:00	0.26	64.6	12.05
10:00-11:00	0.27	63.97	12
11:00-12:00	0.35	65.77	12.32
12:00-13:00	0.35	65.98	12.33
13:00-14:00	0.34	66.22	12.36
14:00-15:00	0.3	66.13	12.35
15:00-16:00	0.27	66.28	12.46
16:00-17:00	0.25	68.37	12.69

Table 3: Room relative and absolute humidity for rpm=1.5

B. Economic analysis of the proposed system vs. conventional vapor compression system

To estimate the economic feasibility and efficiency of the rotating hygroscopic curtain, it will be compared to a conventional vapor compression system that can attain the same indoor conditions (temperature and relative humidity) as that of the rotating curtain system. The conventional vapor compression cycle is assumed to have a coefficient of performance (COP) of 3. It first sub-cools the supply air to reach the required humidity ratio, and then through the use of an electric heating coil, the supply air is reheated to the appropriate supply temperature. For the case study office space considered during the typical summer day, the electric energy required for subcooling and the reheat energy required during one day of operation are shown in Table 4. A total daily electric energy consumption of 4.97 kWh is consumed by the vapor compression cycle in the reheat– subcool process. This amount will not change throughout the considered period of five month since the loads are mostly internal and the supply conditions to the room are the same. In addition the solar radiation profile will not change much over the same period; hence the total electric energy consumption will be 745 kWh for the period of five month. Nevertheless, the power consumption of the electrical motor used to rotate the curtain is 0.035KW, as stated in the motor data sheet, and energy consumption would be 47.25 kWh for a five months operating. The rotating curtain system will induce an electrical energy savings of about 598 kWh.

The cost of electricity in Beirut City is estimated as 0.19 \$/kWh. Therefore the cost of electricity consumption by the vapor compression cycle over the operational period of 5 month per year is calculated to be \$132. As for the rotating curtain system, the price of the motor and the related shaft is about \$200 whereas the textile material cost \$200. Hence the payback period is about 3 years.

Time of the day	Electric energy required for the subcool (kWh)	Reheat electric energy (kWh)	Motor electrical energy (kWh)	Electrical energy savings (kWh)
8:00-9:00	0.231	0.233	0.035	0.429
9:00-10:00	0.247	0.249	0.035	0.461
10:00-11:00	0.256	0.261	0.035	0.482
11:00-12:00	0.337	0.342	0.035	0.644
12:00-13:00	0.337	0.342	0.035	0.644
13:00-14:00	0.324	0.327	0.035	0.616
14:00-15:00	0.290	0.291	0.035	0.546
15:00-16:00	0.258	0.260	0.035	0.483
16:00-17:00	0.191	0.190	0.035	0.346
Total energy (kWh)	2.471	2.495	0.315	4.651

Table 4: Energy loads for the Rotating curtain system and Conventional System

CHAPTER V

CONCLUSION

A mathematical model which simulates the transient moisture uptake of the rotating curtain system is developed and is coupled with a building space conditioned by 100% free cooled fresh air. The moisture curtain model is validated by conducting experiments inside AUB's climatic chamber. The experimental results compare well with the model simulation results. The model is tested on a typical office in the city of Beirut of an area of 42 m^2 . The results indicate that a proper design of a rotating hygroscopic curtain along with a corresponding free cooled air flow can maintain good comfort temperature and relative humidity for a typical office in Beirut without the need of any additional mechanical equipment which requires high grade energy. In fact by adjusting the mass flow rate of cooled air in order to obtain an indoor temperature of 24°C , the average indoor air relative humidity has decreased to an average value of 65.83% when the curtain is rotating at an rpm of 1.5 as compared to a value of 71.1% when the curtain is not rotating.

BIBLIOGRAPHY

- [1] J. Straube. Moisture in buildings. *ASHRAE Journal (January) (2002) 1–5.*
- [2] L. Harriman, G. Brundrett, R. Kittler. Humidity Control Design Guide for Commercial and Institutional Buildings. *ASHRAE, 2001.*
- [3] J. Toftum, A.S. Jorgensen, P.O. Fanger. Upper limits for indoor air humidity to avoid uncomfortably humid skin. *Energy and Buildings 28 (1998) 1–13.*
- [4] Toftum J., and P.O. Fanger. 1999. Air humidity requirements for human comfort. *ASHRAE Transactions 105(2):641-647. Atlanta: American Society of Heating, Refrigerating and Air-Conditioning Engineers, Inc.*
- [5] Fang, L., G. Clausen, and P.O. Fanger. 1998a. Impact of temperature and humidity on the perception of indoor air quality. *Indoor Air 8: 80-90.*
- [6] Fang, L., G. Clausen, and P.O. Fanger. 1998b. Impact of temperature and humidity on the perception of indoor air quality during immediate and longer whole-body exposures. *Indoor Air 8: 276-284.*
- [7] H. R. Trechsel. Moisture control in buildings. *ASTM. 1994 Philadelphia, Pa.: American Society for Testing and Materials.*
- [8] C. Simonson, M. Salonvaara, T. Ojanen. Moisture Content of Indoor Air and Structures in Buildings with Vapor-Permeable Envelopes. Buildings VIII/Moisture Model Validation
- [9] Stegou-Sagia, A and Paigniannis, N. Exergy losses in refrigerating systems. A study for performance comparisons in compressor and condenser . *International Journal of Energy Research, ISSN 0363-907X, 10/2003, Volume 27, Issue 12, pp. 1067 – 1078*

- [10] Goncalves, Pedro; Angrisani, Giovanni; Sasso, Maurizio ; Gaspar, Adelio Rodrigues; Silva, Manuel Gameiro. Exergetic analysis of a desiccant cooling system: searching for performance improvement opportunities. *International Journal of Energy Research*, ISSN 0363-907X, 05/2014, Volume 38, Issue 6, pp. 714 - 727
- [11] Schibuola, Luigi. Humidity control by heat reclaim. *International Journal of Energy Research*, ISSN 0363-907X, 10/2001, Volume 25, Issue 13, pp. 1207 – 1219
- [12] Ghaddar, Nesreen; Ghali, Kamel; Najm, Antoine .Use of a desiccant dehumidification to improve utilization in air-conditioning systems in Beirut. *International Journal of Energy Research*, ISSN 0363-907X, 12/2003, Volume 27, Issue 15, pp. 1317 - 1338
- [13] Hovsopian, R; Vargas, J. V. C; Ordonez, J. C; Krothapalli, A; Parise, J. A. R; Berndsen, J. C. Thermodynamic optimization of a solar system for cogeneration of water heating and absorption cooling. *International Journal of Energy Research*, ISSN 0363-907X, 10/2008, Volume 32, Issue 13, pp. 1210 – 1227
- [14] C. Rode, A. Holm, T. Padfield. A review of humidity buffering in the interior spaces. *Journal of Thermal Envelope and Building Science* 27 (3) (2004) 221–226.
- [15] K. Svennberg. Moisture Buffering in the Indoor Environment. *Building Physics LTH, Print. Report TVBH-1016 Lund, 2006.*
- [16] C. Simonson, M. Salonvaara, T. Ojanen. The effect of structures on indoorhumidity-possibility to improve comfort and perceived air quality. *Indoor Air*12 (3) (2002) 243–251.
- [17] S. Cerolini, M. D’Orazio, C. Di Perna, A. Stazi. Moisture buffering capacity of highly absorbing materials. *Energy and Buildings* 41 (2) (2009) 164–168.

- [18] S. Hameury. Moisture buffering capacity of heavy timber structures directly exposed to an indoor climate: a numerical study. *Building and Environment* 40 (10) (2005) 1400–1412.
- [19] A.H. Holm, H.M. Kunzel, K. Sedlbauer. Predicting indoor temperature and humidity conditions including hygrothermal interactions with the building envelope. *ASHRAE Transactions* 110 (2) (2004) 820–826.
- [20] K. Ghali*, O. Katanani, M. Al-Hindi. Modeling the effect of hygroscopic curtains on relative humidity for spaces air conditioned by DX split air conditioning system. *Energy and Buildings* 43 (2011) 2093–2100
- [21] W.E. Morton, L.W. Hearle. Physical Properties of Textile Fibers. *Heinemann, London, 1975.*
- [22] L. Laret. Use of general models with a small number of parameters. Part 1. Theoretical analysis, in *Proceedings of 7th International Congress of Heating and Air Conditioning CLIMA 2000, Budapest, 1980.*
- [23] ASTM F1868-09, Standard Test Method for Thermal and Evaporative Resistance of Clothing Materials Using a Sweating Hot Plate, *ASTM International, West Conshohocken, PA, 2009, www.astm.org.*
- [24] ISO 11092 (EN 31092). Textiles -- Physiological effects -- Measurement of thermal and water-vapour resistance under steady-state conditions. ISO (International Organization for Standardization); Geneva, Switzerland, 2014.
- [25] K. Keniar, K. Ghali, N. Ghaddar. Study of solar regenerated membrane desiccant system to control humidity and decrease energy consumption in office spaces. *Applied Energy* 138 (2015) 121–132